Applied Physics A (2018) 124:123
https://doi.org/10.1007/s00339-018-1553-1

**Applied Physics A**
**Materials Science & Processing**

# Morphologies of femtosecond laser ablation of ITO thin films using gaussian or quasi-flat top beams for OLED repair

**Hoon-Young Kim[1,2] · Won-Suk Choi[1,2] · Suk-Young Ji[1,2] · Young-Gwan Shin[1,2] · Jin-Woo Jeon[1] · Sanghoon Ahn[1] · Sung-Hak Cho[1,2]**

Received: 23 June 2017 / Accepted: 4 January 2018


**Abstract**
This study compares the ablation morphologies obtained with a femtosecond laser of both Gaussian and quasi-flat top beam profiles when applied to indium tin oxide (ITO) thin films for the purpose of OLED repair. A femtosecond laser system with a wavelength of 1030 nm and pulse duration of 190 fs is used to pattern an ITO thin film. The laser fluence is optimized for patterning at 1.38 J/cm$^2$. The patterned ITO thin film is then evaluated through both optical microscope and atomic force microscope. Ablations with a square quasi-flat top beam are demonstrated using slits with varying $x$–$y$ axes. With the Gaussian beam, the pattern width of the ablated area is shown to range from 9.17 to 9.99 µm when the number of irradiation pulse increases from one to six. In contrast, when slit control is used to obtain a quasi-flat top beam, the ablated pattern width remains constant at 10 µm, despite the increase in the number of pulse. The improved surface roughness is correlated with the quasi-flat top beam through measured Ra values. Furthermore, when using the Gaussian beam, the minimum resolution of the controllable ablation depth on the ITO thin film is found to be 60 nm. In contrast, when the quasi-flat top beam is used, the minimum ablation depth decreases to 40 nm.

## 1 Introduction

Because of the high optical transparency of indium tin oxide (ITO) thin films at visible and near-IR light wavelengths and their high electrical conductivity, these materials are widely used as transparent conducting oxides (TCOs) in the manufacture of optoelectronic devices such as organic light emitting diodes (OLEDs) and organic solar cells [1]. However, some technical issues continue to inhibit the application of ITO thin films; among these are the needs to improve the components' luminous efficiency, reduce their power consumption, and increase their lifetime. In the various industries that use display devices, the methods for controlling the patterning depth of ITO thin films are crucial to improving their optical transmission and electrical conductivity, and reduce their resistance. Enhanced optical transmittance results in reduced power consumption and a subsequent increase in the lifetime of the device [2]. In addition, the resistivity of an ITO pattern should be as low as possible to obtain a high response in display devices such as OLEDs and flat panel displays. Furthermore, well-defined electrode morphologies are important for repairing optoelectronic devices because irregularly patterned morphologies can cause malfunctions or low efficiencies in the devices. Irregularly formed morphologies also generate unfavorable isolations that cause failure when repair of the devices is attempted [3, 4]. Therefore, a uniform morphology of the formed pattern is essential to successfully repair OLEDs.

To form TCOs, a photolithography process has conventionally been used to fabricate ITO thin films on a substrate [5]. Photolithography consists of a wet etching process in acidic solution. However, wet etching processes are often associated with a variety of problems that occur during the manufacturing process, including chemical contamination from the use of hazardous acids, the under-cut effect, swelling of the photoresist, high costs, and damage to the substrate [6]. Therefore, a direct patterning process

✉ Sanghoon Ahn
shahn@kimm.re.kr

✉ Sung-Hak Cho
shcho@kimm.re.kr

[1] Department of Laser and Electron Beam Application, Korea Institute of Machinery & Material (KIMM), 171 Jang-dong, Yuseong-gu, Daejeon 305-343, South Korea

[2] Department of Nano-Mechatronics, Korea University of Science and Technology (UST), 176 Gajung-dong, Yuseong-gu, Daejeon 305-343, South Korea

Published online: 12 January 2018

must be found to replace photolithography. Direct laser patterning is one such dry etching method, and many studies have applied this method to fabricate patterns on TCO films [7–9]. Laser ablation removes materials from a substrate by direct absorption of the laser energy, and can produce the desired combination of detailed patterns by localizing the material removal [10]. Laser processing is advantageous because it reduces the number of steps necessary for traditional processing. Moreover, laser processing has additional advantages, including non-contact processing, high speed, high accuracy, and reduced environmental pollution.

Since the advent of high-intensity femtosecond lasers, the interactions between these ultrashort, high-intensity lasers and several materials has become an area of significant interest [11, 12]. Laser ablation achieves clean patterning without damaging the substrate by locally heating and removing material [13]. In general, ultrashort pulsed lasers induce precise damage thresholds with reduced laser fluence because of their high peak intensity and low pulse energies resulting from the ultrashort pulse duration. These attractive characteristics of femtosecond lasers have enhanced the flexibility of laser micromachining and minimized thermal defects such as micro-cracks and debris; for these reasons, femtosecond lasers have been used as accurate material removal tools in the fabrication of optoelectronic devices [14].

Laser beams with circular Gaussian spatial profiles have typically been used for pattern ablation [15, 16]. A Gaussian beam has significantly different spatial intensity profiles between the center and edge of the focused beam. Recently, some research groups have reported laser ablation of ITO thin films for electrical devices and solar cells using a Gaussian beam [17–19] and Bessel beam [20]. Although the laser patterning of ITO thin films with a Gaussian beam has been previously reported, Gaussian and quasi-flat top beams have not been compared in terms of their respective capacities to minimize ridges and control depth. Optimizing the beam shape to improve the pattern quality is expected to largely determine the repair success yield, which, in turn, is expected to provide a significant advantage in terms of industrial development and cost reductions in the OLED market. Therefore, the experiment reported here compares the results of different beam shapes on the same target to advance the OLED repair industry [21].

This study compares the width variation, surface roughness, and ablation depth of ITO thin films fabricated with Gaussian and quasi-flat top beams by controlling the number of pulses of the femtosecond laser. The quasi-flat top beam originated from a Gaussian beam that was passed through a slit. The morphologies of the ablated areas were characterized with an optical microscope (OM) and atomic force microscopes (AFM).

## 2 Experimental setup

A schematic diagram of the experimental setup is shown in Fig. 1. In the experiments, a commercial regenerative amplified mode-locked Yb:KGW laser (S-Pulse HR, Amplitude Systèmes, France) with a 1030 nm central wavelength, a pulse duration of 190 fs, a repetition rate of 30 kHz, and a maximum pulse energy of 66 µJ was used to pattern the ITO thin films. The pulse energy was calculated after measuring the laser power using a power meter. Depending on the experimental arrangement, either a Gaussian beam profile or a quasi-flat top beam profile was used. Figure 2 shows charge-coupled-device (CCD) camera images of the Gaussian and quasi-flat top beams. The beam $M^2$ quality parameter was 1.2, and the laser beam was focused using an objective lens with 0.42 NA (M Plan Apo NIR 20X, Mitutoyo, Japan). The beam diameter at focus was 2.25 µm. The beam diameter at focus is given by:

$$2\omega_0 = \left(\frac{4\lambda}{\pi}\right)\left(\frac{1}{2\mathrm{NA}}\right)M^2,$$

where $\lambda$ is the wavelength, $\omega_0$ is the beam waist, NA is the numerical aperture, $M^2$ is the beam mode parameter. And, the beam diameter at the output of the laser was 1.36 mm. The laser beam with a Gaussian beam profile was delivered onto the sample through the optical system. The laser beam was focused at 50 µm above the sample to avoid direct ablation on the ITO by the lens used to transfer the slit image. For the experiment with a quasi-flat top beam, after defocusing the beam propagation, the shaped laser beam was

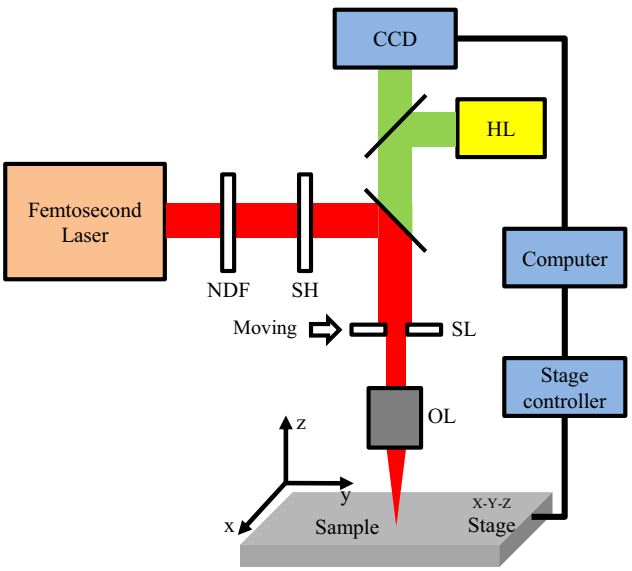


**Fig. 1** Schematic of the femtosecond laser system with a moving slit. *NDF* neutral density filter, *SH* shutter, *HL* halogen lamp, *SL* slit, *OL* objective lens

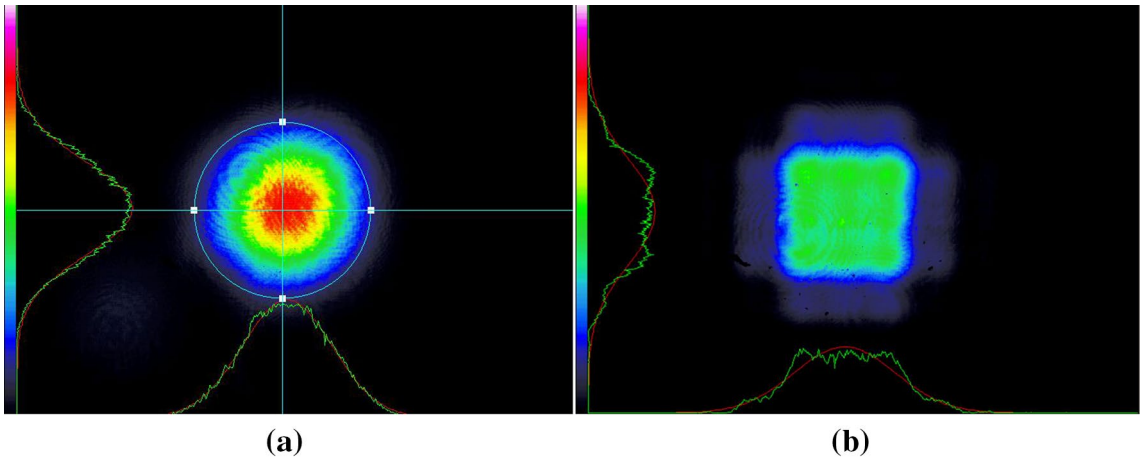


**Fig. 2** CCD camera images of the **a** Gaussian and **b** quasi-flat top beam profiles

irradiated through the slit onto the surface of the ITO thin films. The ITO thin film sample was fixed on a micro-positioning stage controlled by a computer, and the stage could be moved in the *x*-, *y*-, and *z*-axes directions. The pulse energy of the laser was controlled using neutral density filters. The femtosecond laser beam was linearly polarized and had a spatially Gaussian beam profile. As seen in Fig. 1, the Gaussian beam was shaped via the slit to have a quasi-flat top. The quasi-flat top beam had a square shape because of the slit control.

To prepare the samples, ITO thin films with a nominal thickness of 220 nm and a transmittance of 81.5% ($In^2O^3$:$SnO^2$ = 90:10) were deposited onto glass substrates ($20 \times 20 \times 1.2$ $mm^3$) using a DC magnetron sputtering system. The six sides of the glass substrate were optically polished. A sheet resistance of 6.6 Ω/sq was used in the experiments. The surface characteristics of the ablated ITO thin films were observed using OM (MM-20, Nikon, Japan), and cross-sectional samples perpendicular to the ablated ITO thin film patterns were prepared using AFM (NX-10, Park Systems, Korea).

## 3 Results and discussion

Material removal in laser machining occurs when the laser fluence is higher than the damage threshold of the material, which is strongly dependent on the interactions between light and the material's characteristics. In ultrafast laser ablation of any material, a well-defined localization of the photon energy is crucial for removing thin layers from the substrate with minimal thermal effects. For a multilayer target, the damage threshold of each layer is the most important controlling factor for successful selective ablation. A Liu plot is necessary to determine the material's damage threshold with a small number of pulses [22]. The minimum fluence at which machining takes place is calculated by extrapolating the relationship between the fluence and the hole diameter on a Liu plot. To do this, the objective lens is accurately focused on the sample surface, and pulses are generated while the fluence is increased and decreased. The processed sample is then observed with OM, and the diameter of each processed sample is calculated and associated with the fluence at that position.

The experiments in this study were conducted by single-pulse femtosecond irradiation control with both the Gaussian and quasi-flat top beam profiles. Only one pulse irradiation per shot was used. The determined nonlinear relationship between the fluence and hole diameter is shown in Fig. 3. The damage threshold value was calculated from the interaction between the ITO thin film and the femtosecond laser. The measured damage threshold of the ITO thin films in this experiment was 0.14 J/$cm^2$ with a 190-fs pulse width. Ashkenasi et al. reported that the damage threshold of ITO thin films was approximately 0.2 J/$cm^2$ with a pulse width of 200 fs [23]. The difference between these thresholds may be explained by the different etching rate resulting from the distinct nature of each ITO thin film or by a discrepancy in the exact pulse shape of the ultrafast lasers used in the ablation experiment. In our experiment, the measured damage threshold of the glass substrate was 2.1 J/$cm^2$ at a pulse width of 190 fs.

Figures 4 and 5 show the OM images of the morphology of the ablated ITO thin films fabricated with the Gaussian and quasi-flat top beam profiles with a pulse irradiation of 1–6 shots. The widths of the patterns irradiated with the Gaussian and quasi-flat top beam profiles were fixed at approximately 10 μm, primarily because this size corresponds to that required to repair optoelectronic devices. In addition, similar pattern widths were considered necessary

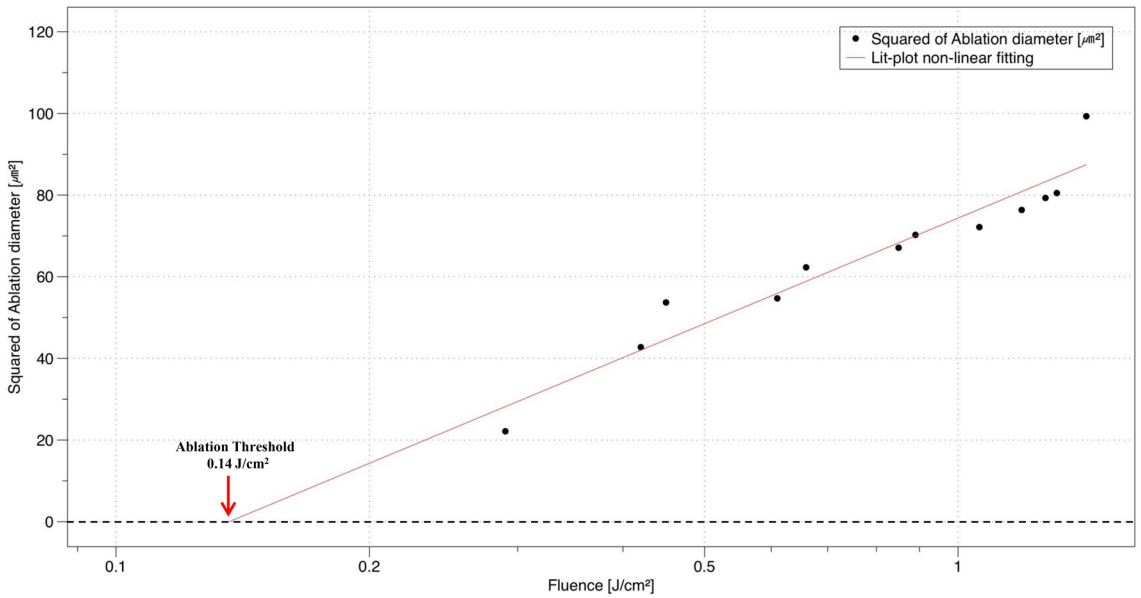


**Fig. 3** ITO thin film damage threshold; experimental results and calculated Liu plot (by nonlinear fitting)

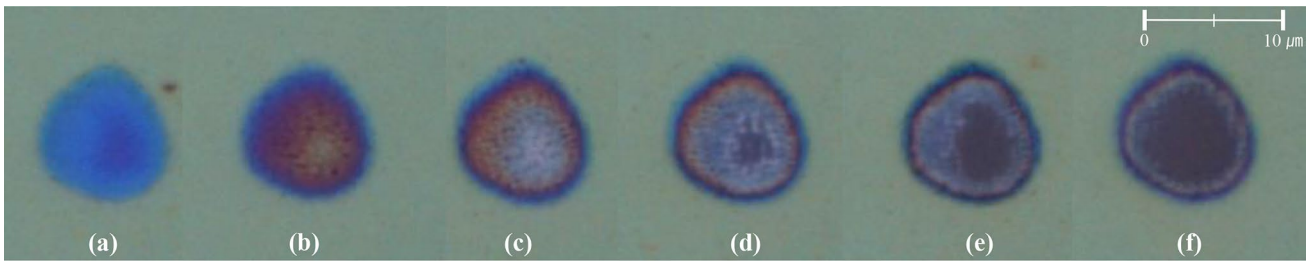


**Fig. 4** OM views of the morphology of the ablated ITO thin film using the Gaussian beam profile with different number of pulse shots: **a** one shot; **b** two shots; **c** three shots; **d** four shots; **e** five shots; and **f** six shots. The experiments were conducted with a single pulse per shot

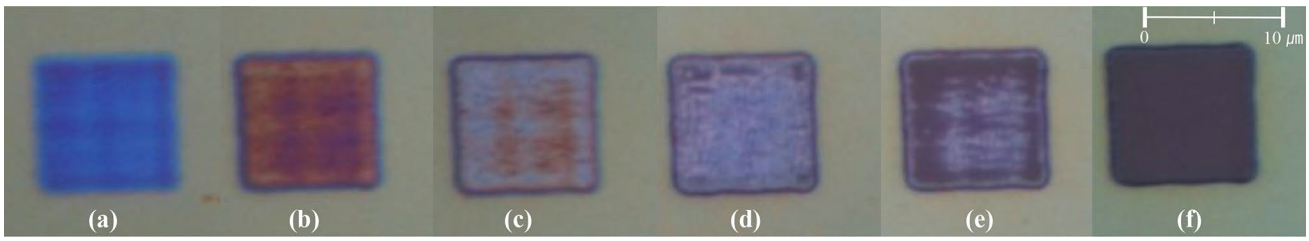


**Fig. 5** OM views of the morphology of the ablated ITO thin film using the quasi-flat top beam profile with different number of pulse shots: **a** one shot; **b** two shots; **c** three shots; **d** four shots; **e** five shots; and **f** six shots. The experiments were conducted with a single pulse per shot

to compare the results of the two beam profiles. In the experiment with the Gaussian beam profile, the fluence of the irradiation laser was fixed at 1.38 J/cm$^2$ to ablate a width of approximately 10 μm. The fluence was less than the damage threshold of the glass substrate (2.1 J/cm$^2$) and higher than that of the ITO thin film (0.14 J/cm$^2$). Figure 4a through f show ablations after a single laser pulse irradiation at a fluence of 1.38 J/cm$^2$ and after increasing the number of laser pulse irradiations with the Gaussian beam profile. This figure clearly shows that, with the irradiated Gaussian beam profile, the width of the ablated pattern increased as the number of laser pulses increased. Furthermore, the center of the circular irradiated region became deeper as the number of irradiated pulses increased.

Figure 5 shows OM images of the experiment with the quasi-flat top beam profile. As shown, the depth of the ablated pattern increased as the number of irradiated pulses increased. However, the Gaussian beam profile produced wider pattern widths with an increasing number of pulses, the width of the pattern ablated with the quasi-flat top beam remained equal to 10 µm even when the number of irradiated pulses increased. Moreover, the entire ablated pattern was evenly distributed, as opposed to that obtained with the Gaussian beam profile. Different colors can be seen in each ablated area in Figs. 4 and 5; the color became darker as the number of irradiation laser pulses increased. Therefore, the selective ablation of ITO layer from the glass substrate was considered to be successfully achieved after irradiation with six laser pulses.

Figure 6 shows the three-dimensional morphologies of the cross-sectional profiles of the Gaussian and quasi-flat top beams after six irradiation pulses. The morphology of the ablated area was obtained with AFM. A cantilever used in non-contact AFM typically has a resonant frequency between 100 and 400 kHz with vibration amplitude of a few nanometers. The three-dimensional morphologies shown in Fig. 6 are the same morphologies shown in Fig. 4f and Fig. 5f. As discussed above when addressing Figs. 4 and 5, selective ablation was achieved with six pulses of irradiation in both the Gaussian and quasi-flat top beam cases.

Figure 7 shows the measured two-dimensional morphologies of the cross-sectional profiles in the ablated area. The measured average depths of the circular ablations after irradiation with the Gaussian beam profile were approximately 60, 120, 190, 210, 220, and 220 nm (black line of Fig. 7a through f, respectively). Moreover, the measured average depths of the square ablations obtained by irradiation with the quasi-flat top beam profile were approximately 60, 105, 140, 190, 210, and 220 nm (redline of Fig. 7a through f, respectively). The two-dimensional depth morphologies in Fig. 7a correspond to those of the same as the samples in Figs. 4a and 5a, respectively.

When we ablated a pattern with a width similar to that used in optoelectronic devices, AFM showed a clear difference in the cross-sectional samples. First, an irregular wall in the ablated pattern was observed the Gaussian beam profile was used; in contrast, there was a reasonably smooth wall in the pattern ablated using slit control. For a number of pulses from one to six, the Ra values indicating the ablated surface roughness were found by AFM to be 28, 48, 70, 88, 97, and 103 nm, respectively, when the Gaussian beam was used. However, the Ra values measured for pulses from one to six using the quasi-flat top beam were 22, 37, 53, 69, 86, and 92 nm, respectively. The Ra value represents the degree of surface roughness in the topography. Therefore, the measured Ra values show a correlation between the improved surface roughness and the quasi-flat top beam. In addition, a relatively clean bottom of the ablated pattern was observed for the quasi-flat top beam irradiation when compared with that of the Gaussian beam irradiation.

Figure 8 shows a graph of the width variation versus pulse number. With the quasi-flat top beam, the ablated pattern width remained constant at 10 µm when the slit control was used, even though the number of irradiated pulses increased. However, with the Gaussian beam, the pattern width of the ablated area ranged from 9.17 to 9.99 µm when the number

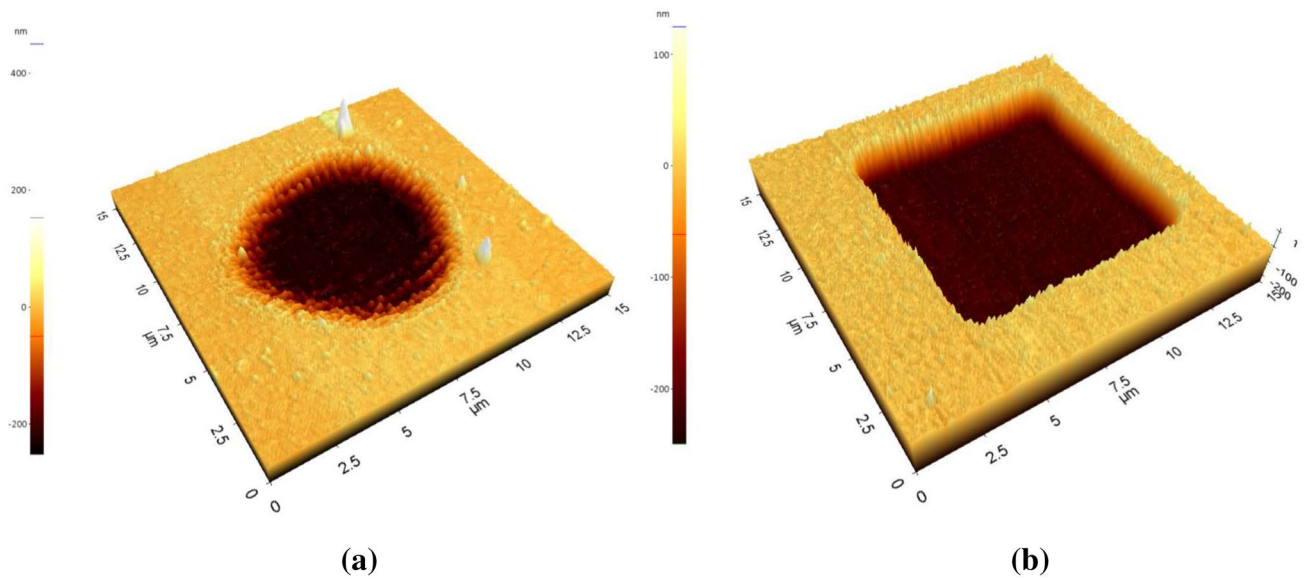


**Fig. 6** Images of the AFM 3D morphology data obtained after six irradiation pulses. The ablation was performed with a femtosecond laser with a single pulse per shot. **a** Gaussian beam profile. **b** Quasi-flat top beam profile

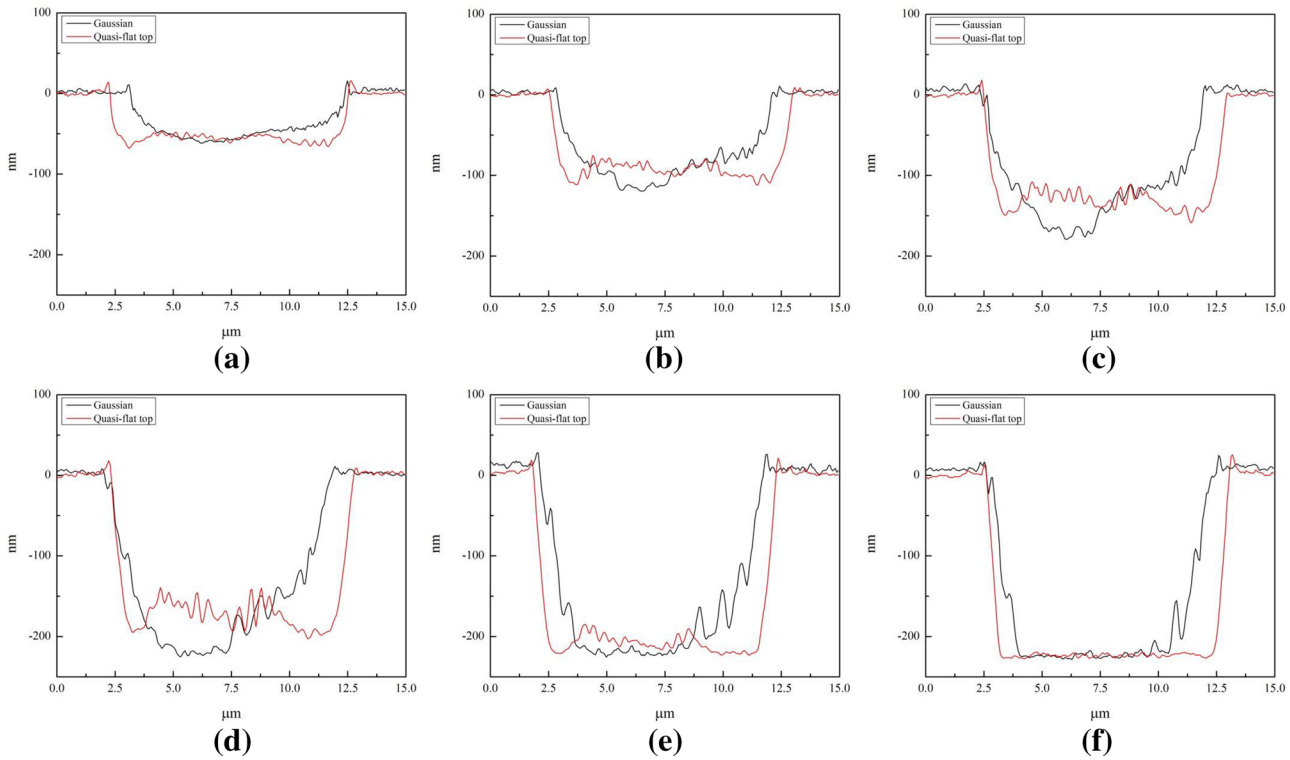


**Fig. 7** Cross-section of the ablated area obtained by AFM after femtosecond laser irradiation. **a** one shot. **b** two shots. **c** three shots. **d** four shots. **e** five shots. **f** six shots

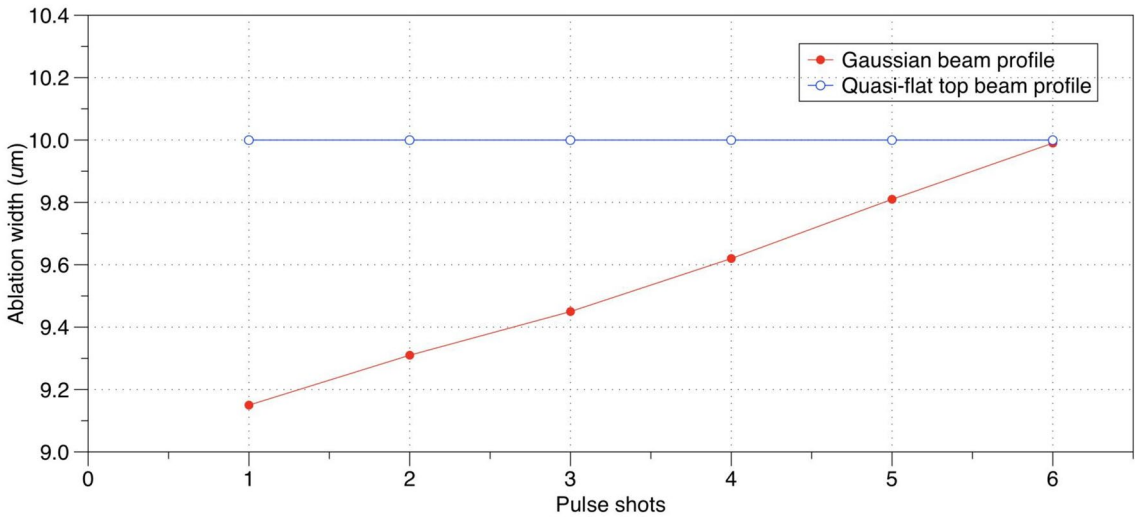


**Fig. 8** Ablation width as a function of the number of pulses

of irradiated pulses increased from one to six. When the Gaussian beam was initially irradiated, no ablation occurred on the pattern edges, and damage occurred only because of the energy distribution of the Gaussian beam. However, damage accumulation on the pattern edges led to ablation as the number of irradiated pulses increased, and the width of the ablated pattern also increased, in contrast with the constant pattern width obtained using the quasi-flat top beam. With the Gaussian beam, the width of the pattern was observed to increase by approximately 0.15 μm with each additional pulse shot; when six laser pulses were irradiated on the ITO thin film, the width reached nearly 10 μm.

Moreover, it was found that the ablation depth increased as the number of pulses increased, as shown in Fig. 9. Using

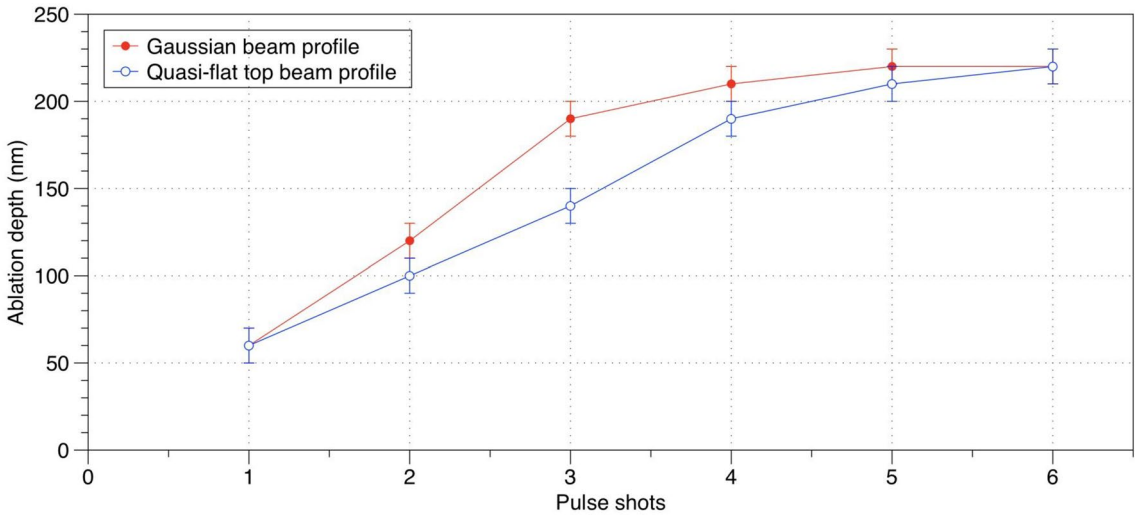


**Fig. 9** Ablation depth as a function of the number of pulses

the Gaussian beam, the minimum resolution of the controllable ablation depth on the ITO thin film was considered to be 60 nm. However, using the quasi-flat top beam, the minimum resolution of the ablation depth was found to be 40 nm. The resolution was defined as the average depth ablated per single pulse irradiation (i.e., the average ablation rate, in depth per pulse). As shown in Fig. 9, the ITO thin film was found to be selectively removed after six pulses of irradiation with the quasi-flat top beam, whereas with the Gaussian beam, selective ablation was achieved after five pulses of irradiation. Furthermore, the quasi-flat top beam was found to allow a more precise pattern depth control than the Gaussian beam. Because the process of repairing OLEDs requires patterning very thin films, the selective ablation must be of high quality and have a high success yield. Therefore, the top-hat-shaped morphology produced by the quasi-flat top beam is considered to be more helpful in OLED repair than the crater-shaped morphology produced by the Gaussian beam.

Although several research groups have reported on ITO thin films, and ablation structures with slits have been reported in several papers on optical waveguides [24], solar cells [21], and electrical devices [7], experimental results comparing ITO thin films ablated using femtosecond lasers with Gaussian and quasi-flat top beam profiles have not been reported. In the optoelectronic industry, the processes must be implemented in precisely the positions for which they were designed, and the ablation sizes must be accurately reproduced. In certain cases, controlling the pattern depth is of particular concern. Based on the analysis of the ablated surface morphologies presented here from the point of view of removal quality, the quasi-flat top beam produced via slit control was found to be preferable to the circular Gaussian beam, because of its capacity to produce higher surface flatness and more finely ablated walls. Moreover, the quasi-flat top beam could be adjusted more precisely when the pattern was processed locally; this technique can, therefore, be applied to improve the performance of optoelectronic devices that require the ablated pattern to be maintained at a constant size.

## 4 Conclusion

In summary, the ablation surface morphologies obtained using a femtosecond laser (1030-nm wavelength, and 190-fs pulse width) with both Gaussian and quasi-flat top beam profiles were compared. A single pulse-controlled femtosecond laser beam was used at a fluence of 1.38 J/cm$^2$. A slit was used to create a square quasi-flat top beam from a Gaussian beam. When the number of irradiation pulses changed from one to six, the ablation depth ranged from 60 to 220 nm. Using the Gaussian beam, the minimum resolution of the controllable ablation depth on the ITO thin film was found to be 60 nm. However, using the quasi-flat top beam, the minimum resolution of the ablation depth was 40 nm. Furthermore, when the number of irradiation pulses increased from one to six, the Ra values indicating the ablated surface roughness were found by AFM to be 28, 48, 70, 88, 97, and 103 nm, respectively, when the Gaussian beam was used. The Ra values measured in the same conditions when the quasi-flat top beam was used were instead of 22, 37, 53, 69, 86, and 92 nm, respectively. When the Gaussian beam was used, the width of the ablated area increased from 9.17 µm to approximately 10 µm, and selective ablation was achieved after five pulses. In contrast, the width of the ablated area when the quasi-flat top beam was used remained constant with the increase in the number of pulses,

and selective ablation of the ITO thin film was achieved after six pulses. The results of this study can be effectively applied to improve the repair and patterning of devices such as displays in the optoelectronic industry.

## References


1. M. Afshar, M. Straub, H. Voellm, D. Feili, K. Koenig, H. Seidel, Opt. Lett **37**, 563 (2012)
2. C.W. Cheng, W.C. Shen, C.Y. Lin, Y.J. Lee, J.S. Chen, Appl. Phys. A **101**, 243 (2010)
3. K.R. Kim, Kor. J. Mat. Res **17**, 352 (2007)
4. H.Y. Kim, J.W. Yoon, W.S. Choi, K.R. Kim, S.H. Cho, Opt. Las. Eng **84**, 44 (2016)
5. M. Hoheisel, A. Mitwalsky, C. Mrotzek, Phys. Stat. Sol **123**, 461 (1991)
6. M.F. Chen, W.T. Hsiao, Y.S. Ho, S.F. Tseng, Y.P. Chen, Thin Solid films **518**, 1072 (2009)
7. Z.H. Li, E.S. Cho, S.J. Kwon, Appl. Surf. Sci **255**, 9846 (2009)
8. G. Raciukaitis, M. Brikas, M. Gedvilas, G. Darcianovas, J. Las. Mic. Nanoeng **2**, 1 (2007)
9. H.W. Choi, D.F. Farson, J. Bovatsek, A. Arai, D. Ashkenasi, Appl. Opt **46**, 5792 (2007)
10. S. Lee, D. Yang, S. Nikumb, Appl. Surf. Sci **253**, 4740 (2007)
11. J.W. Yoon, W.S. Chang, S.H. Cho, Opt. Las. Eng **73**, 40 (2015)
12. C. Park, D.F. Farson, J. Adv. Manu. Tech **83**, 2049 (2016)
13. M. Park, B.H. Chon, H.S. Kim, S.C. Jeoung, D. Kim, J.I. Lee, H.Y. Chu, H.R. Kim, Opt. Las. Eng **44**, 138 (2006)
14. P. Cavallo, R.C. Rodriguez, M. Broglia, D.F. Acevedo, C.A. Barbero, Elec. Acta **116**, 194 (2014)
15. B. Sohn, M.S. Ahsan, D. Yoo, Y.C. Noh, Y.T. Lee, H.K. Choi, J.T. Kim, H.M. Kang, Optik **126**, 4285 (2015)
16. C.W. Cheng, C.Y. Lin, Appl. Sur. Sci **314**, 215 (2014)
17. T.L. Chang, Z.C. Chen, Y.C. Lee, Opt. Exp **20**, 15997 (2012)
18. M.Y. Xu, J. Li, L.D. Lilge, P.R. Herman, Appl. Phys. A **85**, 7 (2006)
19. S.J. Kwon, J. Appl. Phys **47**, 7403 (2008)
20. R. Sahin, I. Kabacelik, Appl. Phys. A **122**, 314 (2016)
21. Q. Bian, X. Yu, B. Zhao, Z. Chang, S. Lei, Opt. Las. Tech **45**, 395 (2013)
22. J.M. Liu, Opt. Lett **7**, 196 (1982)
23. D. Ashkenasi, G. Muller, A. Rosenfeld, R. Stoian, I.V. Hertel, N.M. Bulgakova, E.E.B. Campbell, Appl. Phys. A **77**, 223 (2003)
24. B.J. Luff, J.S. Wilkinson, G. Perrone, Appl. Opt **36**, 7066 (1997)